

Scale Dependent Local Non-Gaussianity from Loops

Jason Kumar¹, Louis Leblond^{2,3}, Arvind Rajaraman⁴

¹*Department of Physics and Astronomy, University of Hawaii,
Honolulu, HI 96822, USA*

²*George P. & Cynthia W. Mitchell Institute for Fundamental Physics,
Texas A&M University, College Station, TX 77843, USA*

³*Perimeter Institute, 31 Caroline St, Waterloo, On, N2L 2Y5, Canada*

⁴*Department of Physics and Astronomy, University of California,
Irvine, CA 92697, USA*

ABSTRACT: We analyze multi-field inflationary systems which yield strongly scale dependent non-Gaussianity with a shape that is very close to the local shape. As in usual multi-field models, the non-Gaussianity arises from the non-linear transfer of scalar field fluctuations to curvature perturbations. Here we consider models in which higher order terms (loops) dominate over the lowest order source of non-linearity. The magnitude of non-Gaussianity depends on an infrared cutoff which is determined by our observational probes measuring non-Gaussianity. In our models, the running is positive and large ($n_{NG} \sim 0.2$) on CMB scales. The magnitude of the bispectrum is maximally of order $\mathcal{O}(100)$, and grows on small scales. This can lead to interesting signals for large scale structure.

KEYWORDS: Effective Field Theory, Cosmology, Inflation.

Contents

1. Introduction	1
2. Scale Dependence from Loops	3
3. Multi-Field Model	4
3.1 The IR cutoff	8
4. The Power Spectrum	9
5. Higher Point Functions	10
5.1 Bispectrum	10
5.2 Trispectrum	14
6. Conclusions	15
A. A Specific Model	17
B. Numerical Evaluation of the Integral	19

1. Introduction

With the advent of precise cosmological data, it is now possible to constrain models of inflation by the measured magnitude and scale-dependence of correlated temperature perturbations in the cosmic microwave background (CMB) and from tracking density perturbations in dark matter from measuring the Large Scale Structure (LSS) of our universe. In these observations, it is found that the primordial perturbations coming from inflation are Gaussian to a remarkable accuracy, in agreement with the predictions of most single field models of inflation.

Non-Gaussianity (NG) can be quantified by the magnitude of the bispectrum denoted f_{NL} (this is usually quoted at the equilateral point in momentum space where all three momenta are equal). For most slow-roll models, f_{NL} is smaller than 1 [1, 2]. By comparison, the most recent constraints from WMAP5 [3] data are $-4 < f_{NL} < 80$ for the local shape and $-125 < f_{NL}^{equi} < 435$ for the equilateral shape [4]. The Planck satellite is expected to improve the bounds to $\Delta f_{NL} < 7$ [5]. There are also a large number of running and upcoming experiments probing LSS

scales (such as LSST, DES, SDSS, etc.) and they may allow us to eventually probe non-Gaussianity on smaller scales.

In this note, we shall consider multi-field models with a large bispectrum (three-point correlation function) that is strongly scale dependent¹. The running is positive (or blue which means that the NG grows as k increases) and can be achieved while keeping the power spectrum nearly scale invariant. It arises from loops (or higher order terms in the local ansatz) and the shape of the bispectrum is very well approximated by the local shape multiplied by a logarithm. We provide a consistent setup where the 1-loop effect dominates the bispectrum while giving a subdominant contribution to the power spectrum, and where higher loop contributions can be neglected. Since the running is positive, we can engineer a set-up where the curvature perturbation on CMB scales are extremely Gaussian while having a detectable NG on LSS scales.

Running NG has already been considered in the context of DBI inflation [13, 14]. This model can have a strong NG signal due to a small and varying sound speed for the inflaton fluctuations [15]. The amplitude of the 3-pt can strongly run with scale if the sound speed varies but the running of the sound speed is exactly cancelled by the quickly varying Hubble constant along the trajectory. This is the key point of this type of model where the potential is steep but the inflaton moves slowly because of a speed limit. This causes the power spectrum to be scale invariant while the bispectrum can run wildly [16, 17].

The prospect of detecting large NG with large scale structure data has spurred much activity recently. LoVerde et al [18] have examined the possibility of using cluster counts and the galaxy bispectrum to constrain running f_{NL} . It was also realized in [19, 20], that NG of the local shape can induce a scale dependence of the galaxy/halo bias (see also [21, 22, 23, 24, 25, 26]). This effect can be easily found in the data and it results in a competitive bound on NG with local shape $-29 < f_{NL} < 70$ [21]. At the time of this writing, there exists no significant experimental bound on the running of NG with scale. Recently, Sefusatti et al [27] argued that Planck could bound n_{NG} , the running of non-Gaussianity, with a precision $\Delta n_{NG} \sim 0.1$ (0.3) for a local (equilateral) shape of non-Gaussianity.

In our models, we find NG with a (nearly) local shape with a scale dependence such that the NG signal grows on small scales. The magnitude of the bispectrum grows with k with a model independent running of $n_{NG} \sim 0.2$ at CMB scale and 0.1 on LSS scale. The strongest constraint on the magnitude of NG arises from n_s . We find that $f_{NL} \sim 100$ can be achieved in principle. We also calculate the trispectrum τ_{NL} , which also runs. Before getting into the details, we summarize the basic idea and results.

¹There has been much recent work in calculating the bispectrum and trispectrum in multi-field inflation, for some recent references see [6, 7, 8, 9, 10, 11, 12].

2. Scale Dependence from Loops

Local shape NG can be obtained in multi-field models of inflation, where each field is Gaussian but a non-linear relation between the inflaton perturbations and curvature perturbations induces NG. The original definition of the local ansatz for the curvature perturbation was done in real space [28]

$$\zeta(\vec{x}, t) = \zeta_{Gauss} + \frac{3}{5} f_{NL} (\zeta_{Gauss}^2 - \langle \zeta_{Gauss}^2 \rangle), \quad (2.1)$$

where ζ_{Gauss} is the Gaussian piece of the curvature perturbation. f_{NL} in this formula is by definition scale invariant. In momentum space, the above ansatz leads to the following bispectrum

$$\begin{aligned} \langle \zeta_{\vec{k}_1} \zeta_{\vec{k}_2} \zeta_{\vec{k}_3} \rangle &= \frac{3}{5} f_{NL} \langle \zeta_{\vec{k}_1} \zeta_{\vec{k}_2} (\zeta \star \zeta)_{\vec{k}_3} \rangle \\ &= (2\pi)^7 \delta^3(\sum \vec{k}_i) \frac{3}{10} f_{NL} (\mathcal{P}^\zeta)^2 \frac{\sum k_i^3}{\prod k_i^3}, \end{aligned} \quad (2.2)$$

where $(\zeta \star \zeta)_{\vec{k}_3}$ denotes a convolution, \mathcal{P}^ζ is the power spectrum (which is assumed to be scale invariant, for simplicity) and $\frac{\sum k_i^3}{\prod k_i^3}$ defines the local shape. Many multi-field models (such as curvatons [29, 30]) have local scale invariant NG of this type. The NG can also be scale dependent even if the shape is nearly local; for example, this is expected to happen when the NG is generated throughout the whole trajectory as opposed to simply at some fixed later time, such as in curvaton models. A particular model with this feature was considered by Byrnes et al [31, 32], where the scale-dependence arises from the dependence of f_{NL} on the (time-dependent) slow-roll and Hubble parameters. In their case, the NG decreases on small scales.

We instead look for scale dependence coming from loops and higher order terms. Indeed, it was realized early on [33] that an additional contribution to the bispectrum in the ansatz Eq. (2.1) comes from

$$\langle \zeta_{\vec{k}_1} \zeta_{\vec{k}_2} \zeta_{\vec{k}_3} \rangle = \left(\frac{3}{5} f_{NL} \right)^3 \langle (\zeta \star \zeta)_{\vec{k}_1} (\zeta \star \zeta)_{\vec{k}_2} (\zeta \star \zeta)_{\vec{k}_3} \rangle. \quad (2.3)$$

This higher order contribution to the bispectrum has a structure similar from a loop contribution as it involves an integral over internal momenta. The integral converges in the UV but contains IR divergences if the power spectrum is nearly scale invariant. One can ‘regulate’ this divergence by introducing an IR cutoff in momenta $1/L^2$.

²These loops have been called c-loops [34]. They must not be confused with q-loops, or loops coming from the expansion of the quantum evolution operator prior to horizon crossing [35]. There has been much discussion recently on the physical significance of the IR divergences in loop calculation in inflation. For c-loops, this IR cutoff is physical and depends on the observational probe and on how we measure the zero mode of curvature perturbations. We will justify this point of view in more detail in Sec. (3.1).

Doing so, the shape of this term is close to local up to a \log [33, 36]

$$\langle \zeta_{\vec{k}_1} \zeta_{\vec{k}_2} \zeta_{\vec{k}_3} \rangle \propto \ln(\text{Min}[k_i]L) \frac{\sum k_i^3}{\prod k_i^3}. \quad (2.4)$$

If this term dominates the bispectrum, we will have a scale dependence with a running of order $n_{NG} \sim \frac{1}{\ln kL}$. As we will show later, the cutoff L is well approximated by the size of the universe today such that $\ln kL \sim 5$ around CMB scale and $n_{NG} \sim 0.2$. The NG grows with scale becoming more important for smaller wavelength. Needless to say this is the interesting case as it gives rise to a stronger signal for LSS.

Recently, Cogollo et al [37] and Rodriguez et al [38] have argued that loops can dominate in a particular 2-brid model. While their idea is very similar to what we propose, their particular model suffers from a problem pointed out in [31]. One of the fields that is assumed to follow a smooth classical trajectory is actually dominated by its quantum fluctuations, undermining part of their analysis.

As we will show, the field that gives rise to NG in our model is also dominated by its quantum fluctuations. But this field plays no role in the inflationary trajectory and there is no inconsistency. We consider multi-field models of hybrid inflation where the inflationary trajectory is dictated by a single field but the surface of reheating (determined by when an extra waterfall/tachyon field starts condensing) fluctuates due to two fields [39, 40] (as originally envisioned by [41, 42] – see also [43, 44, 45] for similar models).

In section 3, we describe the detailed set-up for the model, and describe the infra-red momentum cutoff. In section 4 we compute the power spectrum, and in section 5 we compute the bispectrum and trispectrum. We conclude in section 6 with a discussion of these results.

3. Multi-Field Model

A simple way to move beyond single field slow-roll and generate NG is to have multiple fields. This type of model can quickly become very complicated and in order to simply illustrate the main physical effect of interest (namely large scale dependent NG from loops), we will consider a very simplified set-up. More general models and in-depth analysis of the model we present is left for future work. Consider a model of hybrid inflation with two real light scalar fields (ϕ and χ) and a waterfall field T which ends inflation when it becomes tachyonic and condenses. In this paper, we will consider a rather general action, a more detailed and worked example is given in Appendix A. The action is (we follow the notation of [40]):

$$\begin{aligned} S &= \frac{1}{2} \int \sqrt{g} [M_p^2 R - (\partial\phi)^2 - (\partial T)^2 - (\partial\chi)^2 - 2V] , \\ V &= V_{\text{inf}}(\phi) + V_{\text{hid}}(\chi) + V_{\text{mess}}(\phi, \chi, T) . \end{aligned} \quad (3.1)$$

The only coupling between ϕ and χ are through the tachyon which acts as a mediator or messenger. The form of V_{mess} is taken to be

$$V_{\text{mess}} \propto T^2 f(\phi, \chi) + \mathcal{O}(T^n) \quad ; n > 2 . \quad (3.2)$$

The function f interpolates from large and positive values (in Hubble units) during inflation to negative values after the system crosses a critical line in field space. Therefore during inflation, T has a large positive mass, its vev is driven to zero and its potential vanishes. Because of its large mass, this field will not fluctuate and it can be integrated out of the theory. In this model, inflation ends suddenly when the mass of the tachyon vanishes, which occurs on a line in field space parameterized by

$$f(\phi_e, \chi_e) = 0 , \quad (3.3)$$

where the index “ e ” denotes the value of the fields at the end of inflation. During the inflationary phase, ϕ and χ have no direct coupling. To simplify further, we assume that $V_{\text{hid}}(\chi) \ll V_{\text{inf}}(\phi)$ and we refer to ϕ as the inflaton from now on. The Hubble scale is then approximately given by

$$H^2 \approx \frac{V_{\text{inf}}}{3M_p^2} \quad (3.4)$$

and χ is a “hidden” field during inflation which fluctuates but without much impact on the total energy density of the Universe. Nevertheless, its quantum fluctuations are still important as they will be felt as ripples on the surface of reheating. Indeed, at different point in space, the (slightly) different value of χ_e will mean different critical value ϕ_e for the inflaton resulting in more or less inflation in these different regions. This correlates directly in curvature perturbations (See Fig. (1)) Since the quantum perturbations of χ mainly affect the surface of reheating, this system is well amenable to analysis through the δN (or separable universe) formalism [46]. The idea is that the curvature perturbation on large scales is simply given by the perturbation in the number of efolds for each trajectories

$$\zeta(\vec{x}, t) = \delta N(\vec{x}, t) , \quad (3.5)$$

where the curvature perturbation ζ is given by fluctuations of the scale factor $a(\vec{x}, t) = a(t)e^{\zeta(\vec{x}, t)}$ and the difference in number of efolds is from a initial flat hypersurface to a uniform energy density final hypersurface. This formula does not take into account possible interactions between the various fields inside the horizon (on small scale) and it is only valid after horizon crossing where the evolution of the curvature perturbation is classical³.

³The δN formalism will not account correctly for multi-field effects for modes inside the horizon. In our case, because the fields are uncoupled during inflation, we can solve for $\delta\phi$ and $\delta\chi$ are horizon exit independently and follow the subsequent evolution of ζ with the δN formalism.

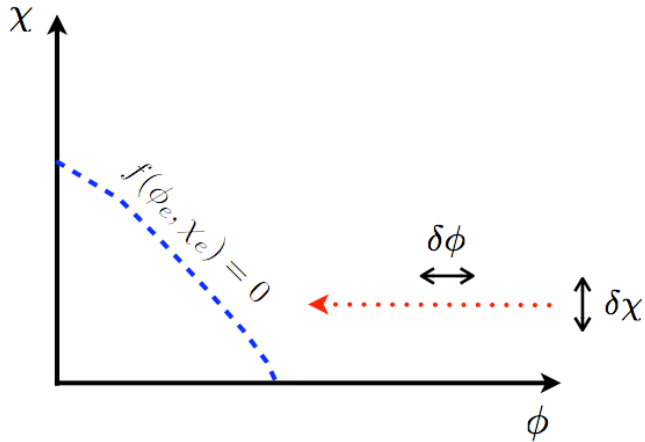


Figure 1: This figure depicts the trajectory in field space. The blue (dashed) line denote the surface of reheating defined by $f(\phi_e, \chi_e) = 0$ and it is assumed to be thin. The classical trajectory is in the ϕ direction (red/dotted line) but both $\delta\phi$ and $\delta\chi$ will induce curvature perturbations.

The surface where inflation ends Eq. (3.3) is not a uniform energy density hypersurface and a correction term must be included as discussed in [47, 44]. The correction term is very small in the hybrid scenario where the potential is very flat and it will be dropped in what follows. The number of efolds is given by $dN = -Hdt$. For the case where the classical trajectory is determined by a single field ϕ , one has

$$N = - \int_{\phi_*}^{\phi_e(\chi)} \frac{H}{\dot{\phi}} d\phi' , \quad (3.6)$$

where the critical value of ϕ depends on the value of the field χ at the end of inflation (we dropped the subscript e and $\chi = \chi_e$ unless otherwise specified⁴) and $*$ refers to horizon crossing for a given mode. By varying $\phi_* \rightarrow \phi_* + \delta\phi$ and then $\phi_e(\bar{\chi} + \delta\chi) = \phi_e + \gamma\delta\chi + \gamma_{,\chi}\delta\chi^2/2 + \dots$ with

$$\gamma(\bar{\chi}) = \frac{\partial\phi_e}{\partial\bar{\chi}} \quad (3.7)$$

where we denote the zero mode of χ by $\bar{\chi}$, that is $\chi(\vec{x}, t) = \bar{\chi}(t) + \delta\chi(\vec{x}, t)$ (for notational simplicity, the bar is omitted in any derivative subscript). We get at second order (using $\frac{H}{\dot{\phi}} = -N'$)

$$\delta N = N'\delta\phi|_* - N'\gamma\delta\chi|_e + \frac{1}{2}N''\delta\phi^2|_* - \frac{1}{2}N'\gamma_{,\chi}\delta\chi^2|_e - \frac{1}{2}N''\gamma^2\delta\chi^2|_e , \quad (3.8)$$

where ' denotes derivatives with respect to ϕ . This can be reproduced using the formula of Vernizzi and Wands [47], for the case $\epsilon^\chi \ll \epsilon^\phi$ albeit they implicitly

⁴The field χ is evolving stochastically and the value of the field at the end of inflation is the sum of all fluctuations created for each mode as they exit the horizon.

assume that all fields obey their equation of motion which is not true here for the field χ . It is simple to show that $N' = \partial N / \partial \phi = 1 / \sqrt{2\epsilon^\phi} M_p$ where the slow-roll parameters are

$$\epsilon^\phi = \frac{1}{2} M_p^2 \left(\frac{V_{\text{inf},\phi}}{V} \right)^2, \quad \epsilon^\chi = \frac{1}{2} M_p^2 \left(\frac{V_{\text{hid},\chi}}{V} \right)^2. \quad (3.9)$$

The terms with N'' involve derivatives of slow-roll parameters and will therefore be suppressed. To simplify the formula and the analysis we will consider the case where the slow-roll parameter at horizon crossing and at the end are equal, $\epsilon_e^\phi = \epsilon_*^\phi$. This is not true in many models and we will discuss at the end how that would affect our results. We thus drop all subscript referring to the time of evaluation. The mean of Eq. (3.8) is non-zero and as it is we will generate a one-pt function. To ensure that the mean is zero we can subtract a constant piece (keeping only the leading terms)

$$\zeta = N' \delta\phi - N' \gamma \delta\chi - \frac{1}{2} N' \gamma_{,\chi} \delta\chi^2 + \frac{1}{2} N' \gamma_{,\chi} \langle \delta\chi^2 \rangle, \quad (3.10)$$

which is of the form Eq. (2.1).

$$\zeta = \zeta_1 + \zeta_2 - \langle \zeta_2 \rangle. \quad (3.11)$$

Note that this series terminates if

1. the function γ is such that $\gamma_{,\chi\chi}$ and higher derivatives are small.
2. N'' and higher derivative contributions are small.

In this type of model, the function γ could be anything and in the case where $\gamma_{,\chi} \delta\chi > \gamma$ the quadratic piece in $\delta\chi$ will dominate over the linear piece (in $\delta\chi$) which ensures that the loop contribution to the bispectrum will dominate

$$\langle \zeta^3 \rangle \propto \gamma_{,\chi}^3 \langle (\delta\chi^2)^3 \rangle, \quad (3.12)$$

as we advocated earlier. In order for the power spectrum to be nearly scale invariant we will still need the $\delta\phi$ piece to be the dominant contribution to the power spectrum. There is no contradiction since the linear perturbation in ϕ does not contribute to the bispectrum (or gives a very small slow-roll suppressed contribution). Furthermore, in the case where the higher derivatives of γ are suppressed, the higher loop contribution can be neglected, ensuring a consistent truncation.

Another important point is that for the loop to dominate, the zero mode of χ at the end of inflation ($\bar{\chi}_e$ which is the mean averaged over the size of the universe at the end of inflation) must be smaller than the $1-\sigma$ deviation value of the perturbation around the mean. Taking the quantum perturbation to be of order $\delta\chi \sim H$, we must have $\bar{\chi}_e < \delta\chi$. This is better seen in a specific model such as the one presented in

Appendix A. There, we use a model where $\phi_e = f(\chi^2)$ such that $\gamma \propto \chi$ and $\gamma_{,\chi} \sim \text{cst}$ and the series truncate. In such models it is clear that the quadratic term dominate over the linear piece when

$$\frac{\gamma_{,\chi}\delta\chi}{\gamma} \sim \frac{\delta\chi}{\chi} > 1. \quad (3.13)$$

It is then clear that the field χ has to behave stochastically and is in no way following a classical equation of motion. The fact that χ has essentially no effect on the inflationary dynamics prior to the reheating tells us that the stochastic behavior is unimportant during inflation. The value of $\bar{\chi}_e$, being stochastic, could have any value and it is therefore a free parameter. Before going into more details of the calculation, we need to discuss the choice of IR cutoff in the loop calculation.

3.1 The IR cutoff

There has been much discussion in the literature about the choice of cutoff that should be used in loop calculations. For the calculation of quantum loops in the in-in formalism (prior to horizon exit), the correlations function of scalars appear to be sensitive to this choice of cutoff, and there is no clear understanding of how this cutoff should be set. But for the c-loops which we consider in this paper, the situation is considerably simpler and there is a natural choice of cutoff [48]. We will define the observed zero modes of the fields ϕ, χ as

$$\phi_0 = \frac{1}{L^3} \int_{-L/2}^{L/2} d^3x \phi, \quad \chi_0 = \frac{1}{L^3} \int_{-L/2}^{L/2} d^3x \chi, \quad (3.14)$$

where L is the largest scale over which we have measured the fields. The perturbations of the fields are then defined as $\delta\phi = \phi - \phi_0, \delta\chi = \chi - \chi_0$.

When computing correlators of δN , we are actually interested in the correlations functions of the perturbations e.g. $\langle \delta\phi_{\vec{k}_1} \delta\phi_{\vec{k}_2} \rangle$. From the definition of the perturbations, we see that the effect of subtracting the zero mode is to remove all Fourier modes with momentum $k > L^{-1}$. Hence $\delta\phi_{\vec{k}} = \phi_{\vec{k}}$ for $k > L^{-1}$, and zero otherwise. Similarly, we find

$$\langle \delta\phi_{\vec{k}_1} \delta\phi_{\vec{k}_2} \rangle = \begin{cases} (2\pi)^3 \delta^3(\vec{k}_1 + \vec{k}_2) 2\pi^2 \frac{\mathcal{P}_*}{k_1^3} & k > L^{-1} \\ 0 & k < L^{-1} \end{cases}. \quad (3.15)$$

The effect is to include a cutoff L^{-1} on any momentum integral. Due to the cutoff, the correlation functions will have an explicit dependence on L . This can be traced back directly to the fact that we are calculating correlation functions of perturbations like $\delta\phi = \phi - \phi_0$, which have a direct dependence on L through ϕ_0 . In this formalism, it is clear that all the dependence on L comes from the variation in the zero mode as a function of L as was discussed in more details in [48] (see also [49]).

To summarize, there is a natural cutoff L determined by the biggest scale on which we are able to measure the background zero mode of curvature. This is maximally the size of the universe today $L \sim 1/H_0$. This coincides with the lowest k perturbations that are possible to observe now. Since there are about 5 efolds between when the lowest observable wavenumber leaves the horizon and when CMB scales leave the horizon, we have $k_{CMB}L \sim e^5$. LSS are about two orders of magnitude greater than CMB scales, giving $k_{LSS}L \sim e^{10}$.

4. The Power Spectrum

We will first consider the two-point function $\langle \zeta_{k_1} \zeta_{k_2} \rangle$. For the scalar fields, we have

$$\begin{aligned} \langle \delta \chi_{\vec{k}}^2 \rangle &= \langle \delta \phi_{\vec{k}}^2 \rangle = (2\pi)^3 \delta^3 \left(\sum_i \vec{k}_i \right) P(k) , \\ P(k) &= \frac{2\pi^2 \mathcal{P}}{k^3} , \end{aligned} \quad (4.1)$$

and we consider a model where these expectation values are approximately constant and where \mathcal{P} is scale invariant (independent of k). We will also assume that any intrinsic 3-pt functions are negligible, $\langle (\delta \phi_k)^n \rangle \approx 0$ and $\langle (\delta \chi_k)^n \rangle \approx 0$ for n odd. In Fourier space the curvature perturbation is given by (from Eq. (3.10))

$$\zeta_{\vec{k}} = N' \delta \phi_{\vec{k}} - N' \gamma \delta \chi_{\vec{k}} - \frac{1}{2} N' \gamma_{,\chi} \int \frac{d^3 \vec{k}'}{(2\pi)^3} \delta \chi_{\vec{k}-\vec{k}'} \delta \chi_{\vec{k}'} + \frac{1}{2} N' \gamma_{,\chi} \langle \delta \chi_{\vec{k}}^2 \rangle , \quad (4.2)$$

The “tree-level” contribution to the power spectrum arises from linear terms in the expansion of δN , and it is easily seen to give

$$\begin{aligned} \langle \zeta_{\vec{k}}^2 \rangle_{tree} &= N'^2 (\langle \delta \phi_{\vec{k}}^2 \rangle + \gamma^2 \langle \delta \chi_{\vec{k}}^2 \rangle) , \\ &= N'^2 (1 + \gamma^2) (2\pi)^3 \delta^3 \left(\sum_i \vec{k}_i \right) P(k) . \end{aligned} \quad (4.3)$$

However, there is also a “one-loop” contribution which arises from the non-linear terms in the δN expansion which leads to

$$\begin{aligned} \langle \zeta_{\vec{k}_1} \zeta_{\vec{k}_2} \rangle_{loop} &= N'^2 \frac{\gamma_{,\chi}^2}{4} \int \frac{d^3 \vec{k}'}{(2\pi)^3} \frac{d^3 \vec{k}''}{(2\pi)^3} \langle \delta \chi_{\vec{k}_1-\vec{k}'} \delta \chi_{\vec{k}'} \delta \chi_{\vec{k}_2-\vec{k}''} \delta \chi_{\vec{k}''} \rangle , \\ &= N'^2 \frac{\gamma_{,\chi}^2}{4} (2\pi)^3 \delta^3 \left(\sum_i \vec{k}_i \right) \int \frac{d^3 k'}{(2\pi)^3} \frac{(2)(2\pi^2 \mathcal{P})^2}{|\vec{k} - \vec{k}'|^3 k'^3} , \end{aligned} \quad (4.4)$$

where the factor of (2) is from the combinatorics. For a scale invariant power spectra \mathcal{P} , the integral is approximately

$$\int_{1/L}^k \frac{d^3 \vec{k}'}{(2\pi)^3} \frac{1}{|\vec{k} - \vec{k}'|^3 k'^3} , \quad (4.5)$$

where we use k as the upper limit because for $k' > k$ the denominator goes as k'^n with $n > 3$, and the integrand drops rapidly. The integrand has two simple poles which give logarithmic divergences. We regulate these by putting an IR cutoff on the integral. Hence for this example, we get

$$\int_{1/L}^k \frac{d^3 \vec{k}'}{(2\pi)^3} \frac{1}{|\vec{k} - \vec{k}'|^3 k'^3} \sim 2 \frac{\ln(kL)}{2\pi^2}. \quad (4.6)$$

This contribution will depend on the IR limit of the momentum integration. This limit is given by the size of the observable universe today, $L \sim H_0^{-1}$ as we discussed in Sec. (3.1). Modes of longer wavelength are already summed in the background value of the field. We thus find

$$\langle \zeta_k^2 \rangle_{loop} = N'^2 \gamma_\chi^2 (2\pi)^3 \delta^3 \left(\sum_i \vec{k}_i \right) \frac{2\pi^2 \mathcal{P}^2 \ln(kL)}{k^3}. \quad (4.7)$$

Combining these terms yields

$$\langle \zeta_k^2 \rangle = (2\pi)^3 \delta^3 \left(\sum_i \vec{k}_i \right) \frac{2\pi^2 \mathcal{P}^\zeta}{k^3}, \quad (4.8)$$

$$= N'^2 (2\pi)^3 \delta^3 \left(\sum_i \vec{k}_i \right) P \left[1 + \gamma^2 + \gamma_\chi^2 \mathcal{P} \ln(kL) \right]. \quad (4.9)$$

We have defined the power spectrum for curvature with the superscript ζ . The spectral index $n_s - 1 = \frac{d \ln \mathcal{P}^\zeta}{d \ln k}$ is

$$n_s - 1 = \frac{\gamma_\chi^2 \mathcal{P}}{1 + \gamma^2 + \gamma_\chi^2 \mathcal{P} \ln kL}. \quad (4.10)$$

Note that the log contribution is positive (blue) and if this is the only contribution, we cannot match to the currently observed value of $n_s \sim 0.96$ [3]. For now, we simply impose that the log contribution contribute no more than a percent correction to n_s

$$\gamma_\chi^2 \mathcal{P} \lesssim 10^{-2}, \quad (4.11)$$

which in turn implies that the non-linear contribution to the 2-point function must be subleading if $\log(kL) \sim 1$.

5. Higher Point Functions

5.1 Bispectrum

We now compute the 3-point function $\langle \zeta_{\vec{k}_1} \zeta_{\vec{k}_2} \zeta_{\vec{k}_3} \rangle$. Again, we find that this correlation function can easily be computed by expanding δN in terms of $\delta\phi$ and $\delta\chi$. Since $\delta\phi$

and $\delta\chi$ are Gaussian fields, the only non-trivial contributions will come from non-linearities in the δN expansion. As in the case of the 2-point function, there is a natural separation into “tree-level” and “loop” contributions [50]. The contribution which is of lowest order in γ, χ is

$$\begin{aligned}\langle \zeta_{\vec{k}_1} \zeta_{\vec{k}_2} \zeta_{\vec{k}_3} \rangle_{tree} &= -\gamma^3 N'^3 \frac{1}{2} \frac{\gamma_{,\chi}}{\gamma}(3) \int \frac{d^3 \vec{k}'}{(2\pi)^3} \langle \delta\chi_{\vec{k}_1} \delta\chi_{\vec{k}_2} \delta\chi_{\vec{k}_3 - \vec{k}'} \delta\chi_{k'} \rangle, \\ &= -\gamma^3 N'^3 (2\pi)^3 \delta^3 \left(\sum_i \vec{k}_i \right) \frac{\gamma_{,\chi}}{\gamma} (2\pi^2 \mathcal{P})^2 \frac{\sum_i k_i^3}{\prod_i k_i^3}.\end{aligned}\quad (5.1)$$

The next term in the γ, χ expansion is

$$\begin{aligned}\langle \zeta_{\vec{k}_1} \zeta_{\vec{k}_2} \zeta_{\vec{k}_3} \rangle_{loop} &= -\gamma^3 N'^3 \frac{1}{8} \frac{\gamma_{,\chi}^3}{\gamma^3} \int \frac{d^3 \vec{k}' d^3 \vec{k}'' d^3 \vec{k}'''}{(2\pi)^9} \langle (\delta\chi_{\vec{k}_1 - \vec{k}'} \delta\chi_{\vec{k}'}) (\delta\chi_{\vec{k}_2 - \vec{k}''} \delta\chi_{\vec{k}''}) (\delta\chi_{\vec{k}_3 - \vec{k}'''} \delta\chi_{\vec{k}'''}) \rangle, \\ &= -\gamma^3 N'^3 (2\pi)^3 \delta^3 \left(\sum_i \vec{k}_i \right) \frac{1}{8} \frac{\gamma_{,\chi}^3}{\gamma^3} \int \frac{d^3 \vec{k}'}{(2\pi)^3} \left(\frac{(2\pi^2 \mathcal{P})^3}{k'^3 |\vec{k}_1 + \vec{k}'|^3 |\vec{k}_2 - \vec{k}'|^3} + 7 \text{ perms} \right), \\ &= -\gamma^3 N'^3 (2\pi)^3 \delta^3 \left(\sum_i \vec{k}_i \right) \frac{1}{8} \frac{\gamma_{,\chi}^3}{\gamma^3} (2\pi^2 \mathcal{P})^3 B(\vec{k}_1, \vec{k}_2, \vec{k}_3).\end{aligned}\quad (5.2)$$

Now the loop integral involves two different momenta

$$B(\vec{k}_1, \vec{k}_2, \vec{k}_3) = \int \frac{d^3 \vec{k}'}{(2\pi)^3} \left(\frac{1}{k'^3 |\vec{k}_1 + \vec{k}'|^3 |\vec{k}_2 - \vec{k}'|^3} + 7 \text{ perms} \right). \quad (5.3)$$

Diagrammatically this is equivalent to a triangular loop of scalars (see Fig. (2)). We note that near the poles at $\vec{k}' = 0, \vec{k}_2, -\vec{k}_1$, we get logarithmic divergences which are cut off by the IR scale L . This logarithmic dependence breaks scale invariance. So our shape B is a function of three variables which we choose to simply be the norm of all three vectors k_1, k_2, k_3 . An estimate of the shape can be obtained by simply evaluating the integral around each poles, cutting off the momentum integration in the infrared at scale $1/L$. So for example, the integrand

$$\int \frac{d^3 \vec{k}'}{(2\pi)^3} \frac{1}{k'^3 |\vec{k}_1 + \vec{k}'|^3 |\vec{k}_2 - \vec{k}'|^3} \quad (5.4)$$

has a pole around $\vec{k}' = 0$, and the integrand falls off rapidly when k' becomes of the same order as k_1 or k_2 . Hence we can approximate the integral around that pole as

$$\int \frac{d^3 \vec{k}'}{(2\pi)^3} \frac{1}{k'^3 |\vec{k}_1 + \vec{k}'|^3 |\vec{k}_2 - \vec{k}'|^3} = \frac{\ln(\text{Min}(k_1, k_2)L)}{2\pi^2 k_1^3 k_2^3} + \dots. \quad (5.5)$$

The same thing can be done for the other poles and for the various permutations. There are also points in parameter space where the integrand has a pole of order

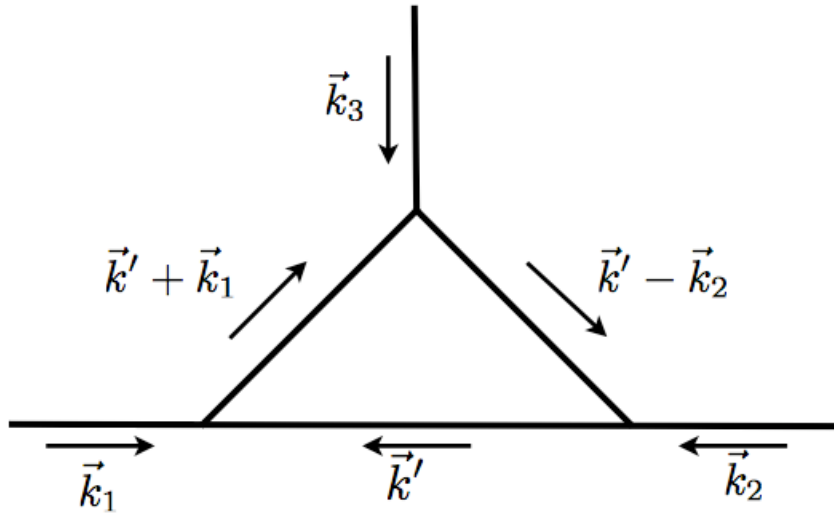


Figure 2: The 1-loop diagram. In our case, each vertex is accompanied by a factor of $N^3\gamma_\chi^3$ while each internal propagator is given by $\frac{2\pi^2\mathcal{P}}{p^3}$. More detailed Feynman rules for use with the δN expansion (which we are not carefully describing here) can be found in [51].

4. These poles occur in the squeezed limit where $\vec{k}_1 = -\vec{k}_2$ and hence $\vec{k}_3 \rightarrow \vec{0}$. This shows that the bispectrum diverges in the squeezed limit, as is usual for the local shape. In principle, we can only measure k to a resolution $\sim 1/L$ and the bispectrum, while large, is finite and of order $L^3/(3k_i^3)$ in this limit. Hence the stronger poles that we have neglected are only important in the squeezed limit and they give contributions of the same order as the log terms in that limit. The full approximative shape is

$$B(k_1, k_2, k_3) \approx \frac{8}{2\pi^2} \left(\frac{\ln(\text{Min}(k_1, k_2)L) + 1/3}{k_1^3 k_2^3} + 2 \text{ perm.} \right). \quad (5.6)$$

The $1/3$ term is only relevant for scales smaller than $k \sim e^{1/3} \frac{1}{L}$. For larger k the shape is very well approximated by

$$B(k_1, k_2, k_3) \approx \frac{8}{2\pi^2} \ln(\text{Min}(k_i)L) \frac{\sum_i k_i^3}{\prod_i k_i^3}. \quad (5.7)$$

We show numerically in Appendix B that this is a good approximation. In Figure (3), we plotted the shape given by Eq. (5.6) in term of the usual variable $x_2 = k_2/k_1$ and $x_3 = k_3/k_1$. When the bispectrum is scale invariant, k_1 is fixed to 1 (arbitrarily) but here we plotted the shape for different value of k_1 . As the figure clearly shows, the graph is very close to local and the magnitude grows as k_1 increases. At the equilateral point $k_1 = k_2 = k_3 \equiv k$, the loop contribution to the bispectrum simplifies

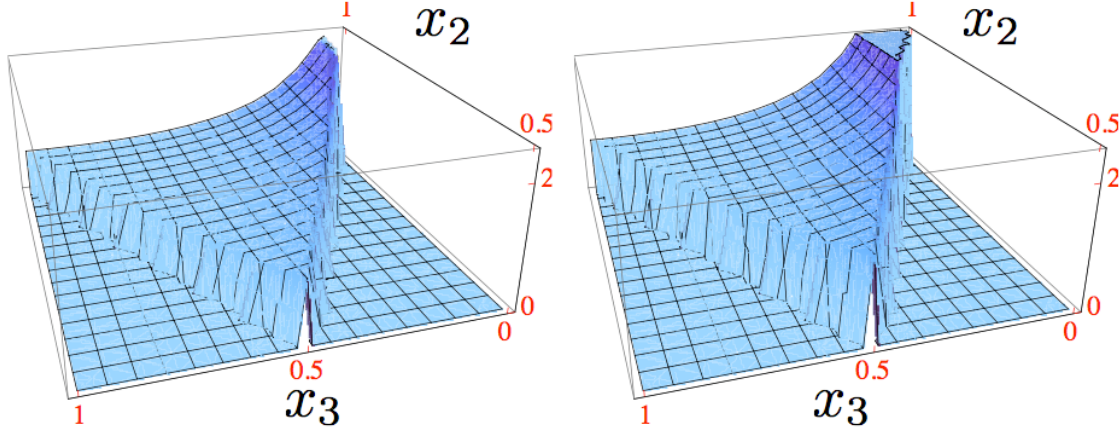


Figure 3: Plot of the approximate shape $B(k_1, k_1 x_2, k_1 x_3) x_2^2 x_3^2 k_1^6$ (with $B(k_1, k_2, k_3)$ given by Eq. (5.6)) in terms of $x_2 = \frac{k_2}{k_1}$ and $x_3 = \frac{k_3}{k_1}$ for $k_1 = 0.5$ (left) and $k_1 = 1.5$ (right). The shape was restricted to be in the quadrant defined by $k_1(1 - x_2) < k_1 x_3 < k_1 x_2$ due to momentum conservation and to avoid overcounting identical triangle configurations (see [52]). The shape is clearly very close to local with the strongest signal in the squeezed limit when $k_3 = k_1 x_3 \rightarrow 0$. The overall magnitude of NG increases with the wavenumber k_1 or as we consider smaller wavelengths.

to

$$\langle \zeta^3 \rangle = -\gamma^3 N'^3 (2\pi)^3 \delta^3 \left(\sum_i \vec{k}_i \right) \frac{\gamma_{,\chi}^3}{\gamma^3} \ln(kL) (2\pi^2)^2 \mathcal{P}^3 \frac{3}{k^6}. \quad (5.8)$$

If we compare the standard parameterization for local non-Gaussianities (Eqns. (2.1) and (2.2)) at the equilateral point to Eq. (5.1) and Eq. (5.8) and using the approximation $\mathcal{P}^\zeta \approx N'^2 \mathcal{P}$, we have

$$f_{NL} \approx -\frac{5}{6} \frac{\gamma^2 \gamma_{,\chi}}{N'} \left(1 + \frac{\gamma_{,\chi}^2}{\gamma^2} \ln(kL) \mathcal{P} \right), \quad (5.9)$$

where the first term is the tree-level contribution, and the second term is the one-loop contribution.

In the case of the two-point function, experimental bounds on the spectral index required the loop-contribution to be subleading. But there is no such requirement for the bispectrum. The loop contribution will dominate if

$$\frac{\gamma_{,\chi}^2}{\gamma^2} \mathcal{P} \ln(kL) > 1. \quad (5.10)$$

In this limit we have

$$|f_{NL}| \approx \frac{5}{6} \frac{(\gamma^2 \mathcal{P})^{\frac{3}{2}}}{N' \mathcal{P}^{\frac{1}{2}}} \ln(kL) \lesssim 100 \ln(kL), \quad (5.11)$$

where we have utilized the bound $\gamma_{,\chi}^2 \mathcal{P} < 10^{-2}$ and the normalization $\mathcal{P}_\zeta^{1/2} \sim N' \mathcal{P}^{1/2} \sim 10^{-5}$ from COBE data. We thus find, in this scenario, that one can easily generate local non-Gaussianity which is not ruled out by WMAP5 and can potentially be probed at Planck. Note that the magnitude of the non-Gaussianity increases logarithmically with momentum, suggesting that non-Gaussianity can have an important impact on the formation of structure at smaller scales. If we define the running of f_{NL} at the equilateral point

$$n_{NG} = \frac{d \ln f_{NL}}{d \ln k} \Big|_{k_i=k} \quad (5.12)$$

one gets in the loop dominated limit

$$n_{NG} \simeq \frac{1}{\ln(kL)} . \quad (5.13)$$

In the limit where non-linearities dominate, the running of f_{NL} is thus independent of N' , γ and $\gamma_{,\chi}$.

5.2 Trispectrum

As in the case of the 3-point function, the only non-vanishing contributions will arise from the non-linear dependence of δN on $\delta\chi$, so we can ignore $\delta\phi$ fluctuations. To simplify notation, we define

$$\zeta_{\vec{k}} = A\delta\chi_{\vec{k}} + B \int \frac{d^3\vec{k}'}{(2\pi)^3} \delta\chi_{\vec{k}-\vec{k}'} \delta\chi_{\vec{k}'} - B \langle \delta\chi_{\vec{k}}^2 \rangle , \quad (5.14)$$

where $A = -N'\gamma$ and $B = -\frac{1}{2}N'\gamma_{,\chi}$. The last term ensures that we only keep the connected part of every diagrams. The tree level contribution (the term of lowest order in B) is

$$\begin{aligned} \langle \zeta_{\vec{k}_1} \zeta_{\vec{k}_2} \zeta_{\vec{k}_3} \zeta_{\vec{k}_4} \rangle &= A^2 B^2 \int \frac{d^3\vec{k}'}{(2\pi)^3} \frac{d^3\vec{k}''}{(2\pi)^3} \langle \delta\chi_{\vec{k}_1} \delta\chi_{\vec{k}_2} \delta\chi_{\vec{k}_3 - \vec{k}'} \delta\chi_{\vec{k}_4 - \vec{k}''} \delta\chi_{\vec{k}'} \delta\chi_{\vec{k}''} \rangle + 5 \text{ perm} , \\ &= (2\pi)^3 4A^2 B^2 \delta^3 \left(\sum \vec{k}_i \right) [P(k_1 + k_3) P(k_1) P(k_2) + 11 \text{ perm}] , \\ &= 4A^2 B^2 (2\pi)^3 \delta^3 \left(\sum \vec{k}_i \right) \frac{T(k_i)}{N'^6} , \end{aligned} \quad (5.15)$$

where we have used that $\mathcal{P}^\zeta \sim N'^2 \mathcal{P}$ and the shape is given by

$$T(k_i) = \left(\frac{(2\pi^2 \mathcal{P}^\zeta)^3}{(k_1 k_{13} k_2)^3} + 11 \text{ perm} \right) \quad (5.16)$$

with the notation $k_{ij} = |\vec{k}_i + \vec{k}_j|$. The magnitude of the trispectrum is usually given by two numbers (τ_{NL} and g_{NL}) corresponding to two distinct shapes:

$$\langle \zeta^4 \rangle = (2\pi)^3 \delta^3 \left(\sum \vec{k}_i \right) \left[\tau_{NL} T(k_i) + \frac{54}{25} g_{NL} (P^\zeta(k_2) P^\zeta(k_3) P^\zeta(k_4) + 3 \text{ perm}) \right] \quad (5.17)$$

The lowest order contribution thus corresponds to $g_{NL} = 0$ and $\tau_{NL} = 4A^2B^2/N^6$. The 1-loop contribution comes from the following term

$$\begin{aligned}\langle \zeta^4 \rangle_{1-loop} &= B^4 \int \frac{d^3 \vec{k}' \cdots d^3 \vec{k}'^{iv}}{(2\pi)^{12}} \langle \delta \chi_{\vec{k}_1 - \vec{k}'} \delta \chi_{\vec{k}'} \cdots \delta \chi_{\vec{k}_4 - \vec{k}'^{iv}} \delta \chi_{\vec{k}'^{iv}} \rangle , \\ &= (2\pi)^3 (16) B^4 \delta^3 \left(\sum \vec{k}_i \right) \left[\int \frac{d^3 k'}{(2\pi)^3} \frac{(2\pi^2 \mathcal{P})^4}{k'^3 |\vec{k}_1 - \vec{k}'|^3 |\vec{k}_1 + \vec{k}_2 - \vec{k}'|^3 |\vec{k}_3 + \vec{k}'|^3} + 5 \text{ perm} \right] .\end{aligned}\quad (5.18)$$

The integral over momentum is difficult in general, so we will only estimate its value at the equilateral point $|k_i| = k$

$$\langle \zeta^4 \rangle_{1-loop} = 16(2\pi)^3 B^4 \delta^3 \left(\sum \vec{k}_i \right) (2\pi^2 \mathcal{P}) \frac{\ln(kL)}{2\pi^2} \frac{T(k_i)}{N^6} \quad (5.19)$$

and thus

$$\begin{aligned}\tau_{NL} &= \frac{4B^2}{N^6} (A^2 + 4B^2 \mathcal{P} \ln(kL)) , \\ &= \frac{\gamma^2 \gamma_{,\chi}^2}{N'^2} \left(1 + \frac{\gamma_{,\chi}^2}{\gamma^2} \mathcal{P} \ln(kL) \right) , \\ g_{NL} &= 0 .\end{aligned}\quad (5.20)$$

We see that the trispectrum is dominated by the non-linear contributions in largely the same regime as the bispectrum. Given the bound from $n_s - 1$, the maximum value for τ_{NL} in this loop dominated regime is

$$\tau_{NL} \sim \frac{\gamma_{,\chi}^4 \mathcal{P}^2}{N'^2 \mathcal{P}} \ln(kL) < 10^6 \ln(kL) . \quad (5.21)$$

Interestingly, the bound from WMAP5 on this parameter is $|\tau_{NL}| < 10^8$ while Planck is expected to improve this bound up to $|\tau_{NL}| < 560$.

6. Conclusions

We have studied a simple class of models in which non-Gaussianity is dominantly produced by higher-order non-linearities in the transfer of fluctuations from the fundamental scalars to the curvature. These higher-order non-linear order contributions are often referred to in the literature as “c-loops”, and can dominate the lowest order “tree-level” contribution in the limit where $\frac{\gamma_{,\chi}^2}{\gamma^2} \mathcal{P} \ln(kL) > 1$, where γ and $\gamma_{,\chi}$ parameterize the non-linear transfer of fluctuations. In particular, $f_{NL} \sim 100$ can be achieved in these models.

We have also found in these models that the magnitude of non-Gaussianity is scale dependent, with $n_{NG} \sim 0.2$ at CMB scales and $n_{NG} \sim 0.1$ at LSS scale. Interestingly, the non-Gaussianity of the bispectrum is stronger at smaller scales,

where it can potentially be observed by large scale structure experiments. The shape of our NG signal is very nearly local. Moreover, this class of models yields a non-trivial trispectrum (parameterized by τ_{NL}) that also runs.

A number of open issues remain. In our model, we have assumed that the slow-roll parameter ϵ is constant throughout inflation. This was necessary in order to have an observable effect from the end of inflation, but it requires tuning and it leads to a very flat power spectrum. It would be interesting to either relax this assumption in our scenarios or to look at a completely different set-up where the NG is not generated at the end of inflation. We expect that we can relax this assumption since we could have a case where f_{NL} is very small on CMB scales but grows to be detectable on LSS scales. We note though that D-term inflation with a Coleman-Weinberg potential (as illustrated in Appendix A) has a natural regime with the required flat potential, $\epsilon_e \sim \epsilon_f$. From an effective field theory point of view (and from string theory models such as [40, 53]), the real tuning is in keeping all other allowed terms (such as a mass term for ϕ) subdominant to the Coleman-Weinberg potential.

We have also assumed that the fundamental scalars (ϕ and χ) are Gaussian, and that all non-Gaussianity is induced by the non-linear transfer of $\delta\chi$ fluctuations to the curvature. Non-trivial NG can also arise from non standard kinetic terms, or a steep potential for χ (which unlike the inflaton does not have to satisfy slow-roll conditions). Loop corrections then have a richer structure although the basic idea remains the same. Of particular interest are models like DBI inflation where the spectral index is nearly one and entropy modes being converted to curvature at the end of inflation can also be observable [54]. This scenario has been analyzed recently in [55] based on methods developed in [56, 57] (see also [58][59]) and a mixture of equilateral and local NG has been found. It would be interesting to consider the regime where the loop dominate in this kind of models.

Acknowledgments

We are particularly thankful to Bhaskar Dutta for early collaboration on this project. We are grateful to Niayesh Afshordi, Sarah Shandera, Martin Sloth, Xerxes Tata and Andrew Tolley for useful discussions. L.L. would like to thank the organizers of the workshop on Effective Field Theory of Inflation at the Perimeter Institute and of the Phenomenology workshop at Cooks Branch Conservancy where part of this work was presented. L.L. would also like thank the KITP and the Aspen Institute for their hospitality. LL is supported in part by NSF Grant No. PHY-0505757. AR is supported in part by NSF Grant No. PHY-0653656. This research was supported in part by Perimeter Institute for Theoretical Physics. Research at Perimeter Institute is supported by the Government of Canada through Industry Canada and by the province of Ontario through the Ministry of Research & Innovation.

A. A Specific Model

The discussion in the text is very general and the ultimate goal of having dominant loop contribution in the bispectrum inducing a large running may be achievable in a variety of ways. Here we illustrate the necessary ingredients with a specific model (based on [39]). Take an inflationary potential

$$V_{\text{inf}} = \frac{g^2 \xi^2}{2} \left[1 + \frac{g^2}{16\pi^2} V_{CW}(x) \right], \quad (A.1)$$

$$V_{CW}(x) = (x^2 + 1)^2 \ln(x^2 + 1) - 2x^4 \ln x^2 + (x^2 - 1)^2 \ln(x^2 - 1) - 4 \ln 2,$$

where $x^2 = \frac{\lambda^2 \phi^2}{g^2 \xi^2}$, ξ has mass dimension 2 and λ and g are dimensionless couplings. The reader will recognize this as the Coleman-Weinberg potential. There is a regime in parameter space where the inflaton does not move very much with

$$\phi_*^2 \sim \phi_e^2 = \frac{g^2 \xi}{\lambda^2} \quad (A.2)$$

and the slow-roll parameter is also nearly constant⁵

$$\epsilon^\phi = \left(\frac{g^2 \ln 2}{\pi^2 \phi} \right)^2 \frac{M_p^2}{2} \sim \frac{\lambda^2 g^2 (\ln 2)^2 M_p^2}{2\pi^4 \xi}. \quad (A.3)$$

The ϕ and χ power spectrum are simply given by $\mathcal{P} = \frac{H^2}{(2\pi)^2}$ and they will remain approximately constant until the end of inflation if η_ϕ and η_χ are much smaller than 1. Now consider a simple potential for χ

$$V_{\text{hid}} = \nu^2 \chi^4 / 4. \quad (A.4)$$

This potential drives χ to 0 but the field will fluctuate and acquire some stochastic value $\bar{\chi}$ which in general will be non-zero (although small). The tachyon potential is of the form Eq. (3.2) with the surface of reheating defined by

$$0 = f(\phi_e, \chi_e) = -g^2 \xi + \lambda^2 \phi_e^2 + \beta \chi_e^2. \quad (A.5)$$

We choose a model such that $\chi_e = \bar{\chi}_e + \delta\chi \ll \phi_e$. Since the function f is quadratic in both fields, the transfer function is simply

$$\gamma = \left. \frac{\partial \phi_e}{\partial \chi} \right|_e = -\frac{\beta}{\lambda^2} \frac{\bar{\chi}_e}{\phi_e}, \quad (A.6)$$

and $\gamma_{,\chi} \sim \frac{\gamma}{\chi}$ while $\gamma_{,\chi\chi} \sim 0$. Note that γ and $\gamma_{,\chi}$ can both be either sign depending on β . The curvature power spectrum is (from Eq. (4.8))

$$\mathcal{P}_\zeta = \frac{H^2}{2(2\pi)^2 \epsilon^\phi M_p^2} \left(1 + \gamma^2 + \frac{\gamma_{,\chi}^2 H^2 \ln kL}{(2\pi)^2} \right). \quad (A.7)$$

⁵By integrating the EoM of motion of ϕ , in the limit $x \rightarrow 1$, one can check that $\phi_* \sim \phi_e$ is a good approximation as long as $\frac{\xi}{M_p^2 \lambda^2} \gg \frac{2\sqrt{2} \ln 2 N_e}{\pi^2}$ where N_e is the number of efolds between horizon crossing and the surface of reheating.

We are interested in the regime where

$$1 > \frac{\gamma_{,\chi}^2 H^2 \ln kL}{(2\pi)^2} > \gamma^2 \quad (\text{A.8})$$

and where the power spectrum \mathcal{P}^ζ , f_{NL} and τ_{NL} are well approximated by

$$\begin{aligned} \mathcal{P}_\zeta &\sim \frac{\pi^2}{6} \frac{\xi^3}{(2\ln 2)^2 \lambda^2 M_p^6}, \\ f_{NL} &= \frac{5 \ln 2 \beta^3 H^2 M_p^2 \ln kL}{6\pi^2 \lambda^2 g^2 (2\pi)^2 \xi^2}, \\ \tau_{NL} &= \frac{\beta^4 M_p^4 H^2 \ln kL}{8\pi^4 (2\pi)^2 \lambda^2 g^2 \xi^3}. \end{aligned} \quad (\text{A.9})$$

Note that none of these observables depend on the precise value of $\bar{\chi}$ at the end of inflation although in order for the loop contribution it must be that the average value of the zero mode of χ at the end of inflation is smaller than H . We show a point in parameter space (see Table (1)) where all the conditions mentioned in this section are respected.

g	λ	β	ξ/M_p^2
10^{-3}	2×10^{-4}	0.1	2.98×10^{-6}

Table 1: A point in parameter space. λ was first chosen and ξ was solved for by matching to COBE data. The parameter g is then constrained such that $\phi < M_p$ by at least two order of magnitude. β is a free parameters that determine the magnitude of NG. The stochastic value of χ at the end of inflation in this model is less than H although none of the observables depend on its precise value. One can check that for this choice of parameters: $\lambda^2 \phi_e \gg \lambda' \chi^2$, $\frac{\gamma_{,\chi}^2 H^2 \ln kL}{(2\pi)^2} = 0.03$ and $\gamma^2 \sim 0.001$. Also for this choice of parameter the potential is very flat with $\epsilon_*^\phi \sim \epsilon_e^\phi \sim 10^{-11}$ while $\epsilon_e^\chi \sim 10^{-29}$ (for $\nu^2 \sim 10^{-2}$ giving $\eta_\chi \sim 10^{-2}$).

	$\ln kL$	\mathcal{P}_ζ	f_{NL}	τ_{NL}	$n_s - 1$	n_{NG}
CMB scales	~ 5	2×10^{-9}	1.6	1152	0.004	0.2
LSS scales	~ 10	2×10^{-9}	62	4.5×10^4	0.004	0.1

Table 2: Predicted value for various parameters. This point was deliberately chosen to illustrate the possibility of having a non-observable level of NG at CMB scale but with a very detectable signal for LSS.

As can be seen from Table (2), this simple model can lead to interesting observational signatures whereas the CMB is very Gaussian, but significant NG appears for large scale structure. On the other hand, not everything is perfect since the spectral index is nearly one in tension with the most current WMAP5 data. This is direct consequence of working with a model where $\epsilon_*^\phi \sim \epsilon_e^\phi$. If this assumption is relaxed,

a running will be induced but the non-Gaussian signal coming from the end of inflation will also be reduced. This can potentially be compensated by varying other parameters but this required more detailed analysis keeping track of the time of evaluation for each quantity. We leave this for further work. Note also that the tension between $n_s \sim 1$ and WMAP5 data can also be reduced if cosmic strings (which are generically produce in these hybrid models) contribute to the density perturbation spectrum [60]. The cosmic strings will add their own source of NG which will further constrain the model [61].

B. Numerical Evaluation of the Integral

The integral

$$B(\vec{k}_1, \vec{k}_2, \vec{k}_3) = \int \frac{d^3 k'}{(2\pi)^3} \left(\frac{1}{k'^3 |\vec{k}_1 + \vec{k}'|^3 |\vec{k}_2 - \vec{k}'|^3} + 7 \text{ perms} \right) \quad (\text{B.1})$$

can be evaluated numerically in Mathematica. There are three poles in the integrand, and the IR cutoff discussed in Sec. (3.1) is most easily implemented by setting the integrand to zero whenever k' is within $1/L$ of a pole.

On general grounds, one expects that the integral is can be written as

$$B(\vec{k}_1, \vec{k}_2, \vec{k}_3) = \sum_i \ln(k_i L) F_0^i(|\vec{k}_1|, |\vec{k}_2|) + F_1(|\vec{k}_1|, |\vec{k}_2|) + \dots, \quad (\text{B.2})$$

where the neglected terms contain powers of $1/k_i L$. For momenta relevant to CMB, these terms are very small. Note that both F_0 and F_1 are homogeneous Lorentz invariant functions of the external momenta with degree -6 (i.e., are scale-invariant), and thus are completely determined by the norms of any two of the momenta.

As argued in Sec. (5.1), the leading term is dominated by the poles of the integrand, and we expect it to be of the form

$$\sum_i \ln(k_i L) F_0^i(\vec{k}_1, \vec{k}_2, \vec{k}_3) = \frac{8}{2\pi^2} \frac{\sum_i \ln(\text{Min}(k_{\alpha \neq i} L) k_i^3)}{\left(\prod_j k_j^3 \right)}. \quad (\text{B.3})$$

Because $F_{0,1}$ are scale-invariant, we can numerically integrate the shape at various scales and fit the result to our ansatz in order to determine the magnitude of $F_{0,1}$.

For example, we numerically integrated B at the equilateral limit $k_i = k$ for various values of k near the range $kL \approx 150$, and we fitted the results to the ansatz $B(k, k, k) \times (kL)^6 = c_0 \ln(kL) + c_1$. This fit yielded the expected $c_0 \sim \frac{12}{\pi^2}$, where the second term c_1 was $\sim 5\%$ of the first term. Similarly, one can integrate B for several external momenta in the squeezed limit where $k_1 L = k_{small} L \sim 150$ and $k_2 L = k_3 L = k_{big} L \sim 10000$. Since the local shape should dominate in this limit, one would fit this to $B(k_{small}, k_{big}, k_{big}) \times (k_{small} L)^3 (k_{big} L)^3 \sim d_0 \ln(k_{small} L) + d_1$. Again as expected, one finds $d_0 \sim \frac{8}{\pi^2}$, where the non-logarithmic term d_1 was $\sim 8\%$ of the logarithmic term. We conclude that the logarithm captures the leading behavior.

References

- [1] J. M. Maldacena, *Non-gaussian features of primordial fluctuations in single field inflationary models*, *JHEP* **05** (2003) 013, [[astro-ph/0210603](#)].
- [2] V. Acquaviva, N. Bartolo, S. Matarrese, and A. Riotto, *Second-order cosmological perturbations from inflation*, *Nucl. Phys.* **B667** (2003) 119–148, [[astro-ph/0209156](#)].
- [3] **WMAP** Collaboration, E. Komatsu *et. al.*, *Five-year wilkinson microwave anisotropy probe (wmap) observations:cosmological interpretation*, *Astrophys. J. Suppl.* **180** (2009) 330–376, [[0803.0547](#)].
- [4] L. Senatore, K. M. Smith, and M. Zaldarriaga, *Non-Gaussianities in Single Field Inflation and their Optimal Limits from the WMAP 5-year Data*, [0905.3746](#).
- [5] A. Cooray, D. Sarkar, and P. Serra, *Weak Lensing of the Primary CMB Bispectrum*, *Phys. Rev.* **D77** (2008) 123006, [[0803.4194](#)].
- [6] D. Langlois, F. Vernizzi, and D. Wands, *Non-linear isocurvature perturbations and non- Gaussianities*, *JCAP* **0812** (2008) 004, [[0809.4646](#)].
- [7] X. Gao, M. Li, and C. Lin, *Primordial Non-Gaussianities from the Trispectra in Multiple Field Inflationary Models*, [0906.1345](#).
- [8] F. Arroja, S. Mizuno, and K. Koyama, *Non-gaussianity from the bispectrum in general multiple field inflation*, *JCAP* **0808** (2008) 015, [[0806.0619](#)].
- [9] Q.-G. Huang, *The Trispectrum in the Multi-brid Inflation*, *JCAP* **0905** (2009) 005, [[0903.1542](#)].
- [10] Q.-G. Huang, *A geometric description of the non-Gaussianity generated at the end of multi-field inflation*, *JCAP* **0906** (2009) 035, [[0904.2649](#)].
- [11] C. T. Byrnes and G. Tasinato, *Non-Gaussianity beyond slow roll in multi-field inflation*, *JCAP* **0908** (2009) 016, [[0906.0767](#)].
- [12] D. Battefeld and T. Battefeld, *On Non-Gaussianities in Multi-Field Inflation (N fields): Bi- and Tri-spectra beyond Slow-Roll*, [0908.4269](#).
- [13] M. Alishahiha, E. Silverstein, and D. Tong, *Dbi in the sky*, *Phys. Rev.* **D70** (2004) 123505, [[hep-th/0404084](#)].
- [14] E. Silverstein and D. Tong, *Scalar speed limits and cosmology: Acceleration from deceleration*, *Phys. Rev.* **D70** (2004) 103505, [[hep-th/0310221](#)].
- [15] X.-G. Chen, *Running non-gaussianities in dbi inflation*, [astro-ph/0507053](#).
- [16] C. Armendariz-Picon and E. A. Lim, *Scale invariance without inflation?*, *JCAP* **0312** (2003) 002, [[astro-ph/0307101](#)].

- [17] J. Khoury and F. Piazza, *Rapidly-Varying Speed of Sound, Scale Invariance and Non- Gaussian Signatures*, *JCAP* **0907** (2009) 026, [[0811.3633](#)].
- [18] M. LoVerde, A. Miller, S. Shandera, and L. Verde, *Effects of scale-dependent non-gaussianity on cosmological structures*, [arXiv:0711.4126 \[astro-ph\]](#).
- [19] N. Dalal, O. Dore, D. Huterer, and A. Shirokov, *The imprints of primordial non-gaussianities on large- scale structure: scale dependent bias and abundance of virialized objects*, *Phys. Rev.* **D77** (2008) 123514, [[0710.4560](#)].
- [20] S. Matarrese and L. Verde, *The effect of primordial non-Gaussianity on halo bias*, *Astrophys. J.* **677** (2008) L77, [[0801.4826](#)].
- [21] A. Slosar, C. Hirata, U. Seljak, S. Ho, and N. Padmanabhan, *Constraints on local primordial non-gaussianity from large scale structure*, *JCAP* **0808** (2008) 031, [[0805.3580](#)].
- [22] N. Afshordi and A. J. Tolley, *Primordial non-gaussianity, statistics of collapsed objects, and the integrated sachs-wolfe effect*, *Phys. Rev.* **D78** (2008) 123507, [[0806.1046](#)].
- [23] P. McDonald, *Primordial non-gaussianity: large-scale structure signature in the perturbative bias model*, *Phys. Rev.* **D78** (2008) 123519, [[0806.1061](#)].
- [24] U. Seljak, *Extracting primordial non-gaussianity without cosmic variance*, *Phys. Rev. Lett.* **102** (2009) 021302, [[0807.1770](#)].
- [25] A. Taruya, K. Koyama, and T. Matsubara, *Signature of primordial non-gaussianity on matter power spectrum*, *Phys. Rev.* **D78** (2008) 123534, [[0808.4085](#)].
- [26] M. Grossi *et. al.*, *Large-scale non-Gaussian mass function and halo bias: tests on N-body simulations*, [0902.2013](#).
- [27] E. Sefusatti, M. Liguori, A. P. S. Yadav, M. G. Jackson, and E. Pajer, *Constraining running non-gaussianity*, [0906.0232](#).
- [28] E. Komatsu and D. N. Spergel, *Acoustic signatures in the primary microwave background bispectrum*, *Phys. Rev.* **D63** (2001) 063002, [[astro-ph/0005036](#)].
- [29] A. D. Linde and V. F. Mukhanov, *Nongaussian isocurvature perturbations from inflation*, *Phys. Rev.* **D56** (1997) 535–539, [[astro-ph/9610219](#)].
- [30] D. H. Lyth and D. Wands, *Generating the curvature perturbation without an inflaton*, *Phys. Lett.* **B524** (2002) 5–14, [[hep-ph/0110002](#)].
- [31] C. T. Byrnes, K.-Y. Choi, and L. M. H. Hall, *Large non-gaussianity from two-component hybrid inflation*, *JCAP* **0902** (2009) 017, [[0812.0807](#)].
- [32] C. T. Byrnes, K.-Y. Choi, and L. M. H. Hall, *Conditions for large non-Gaussianity in two-field slow- roll inflation*, *JCAP* **0810** (2008) 008, [[0807.1101](#)].

- [33] D. H. Lyth and Y. Rodriguez, *The inflationary prediction for primordial non-gaussianity*, *Phys. Rev. Lett.* **95** (2005) 121302, [[astro-ph/0504045](#)].
- [34] D. H. Lyth and D. Seery, *Classicality of the primordial perturbations*, *Phys. Lett.* **B662** (2008) 309–313, [[astro-ph/0607647](#)].
- [35] S. Weinberg, *Quantum contributions to cosmological correlations*, *Phys. Rev.* **D72** (2005) 043514, [[hep-th/0506236](#)].
- [36] L. Boubekeur and D. H. Lyth, *Detecting a small perturbation through its non-Gaussianity*, *Phys. Rev.* **D73** (2006) 021301, [[astro-ph/0504046](#)].
- [37] H. R. S. Cogollo, Y. Rodriguez, and C. A. Valenzuela-Toledo, *On the Issue of the ζ Series Convergence and Loop Corrections in the Generation of Observable Primordial Non- Gaussianity in Slow-Roll Inflation. Part I: the Bispectrum*, *JCAP* **0808** (2008) 029, [[0806.1546](#)].
- [38] Y. Rodriguez and C. A. Valenzuela-Toledo, *On the Issue of the ζ Series Convergence and Loop Corrections in the Generation of Observable Primordial Non- Gaussianity in Slow-Roll Inflation. Part II: the Trispectrum*, [0811.4092](#).
- [39] B. Dutta, L. Leblond, and J. Kumar, *Tachyon mediated non-gaussianity*, *Phys. Rev.* **D78** (2008) 083522, [[0805.1229](#)].
- [40] B. Dutta, J. Kumar, and L. Leblond, *An inflationary scenario in intersecting brane models*, *JHEP* **07** (2007) 045, [[hep-th/0703278](#)].
- [41] L. Alabidi and D. Lyth, *Curvature perturbation from symmetry breaking the end of inflation*, [astro-ph/0604569](#).
- [42] L. Alabidi, *Non-gaussianity for a two component hybrid model of inflation*, *JCAP* **0610** (2006) 015, [[astro-ph/0604611](#)].
- [43] F. Bernardeau and T. Brunier, *Non-gaussianities in extended d-term inflation*, *Phys. Rev.* **D76** (2007) 043526, [[0705.2501](#)].
- [44] M. Sasaki, *Multi-brid inflation and non-gaussianity*, *Prog. Theor. Phys.* **120** (2008) 159–174, [[0805.0974](#)].
- [45] A. Naruko and M. Sasaki, *Large non-Gaussianity from multi-brid inflation*, *Prog. Theor. Phys.* **121** (2009) 193–210, [[0807.0180](#)].
- [46] M. Sasaki and E. D. Stewart, *A general analytic formula for the spectral index of the density perturbations produced during inflation*, *Prog. Theor. Phys.* **95** (1996) 71–78, [[astro-ph/9507001](#)].
- [47] F. Vernizzi and D. Wands, *Non-Gaussianities in two-field inflation*, *JCAP* **0605** (2006) 019, [[astro-ph/0603799](#)].

[48] D. H. Lyth, *The curvature perturbation in a box*, *JCAP* **0712** (2007) 016, [[0707.0361](#)].

[49] K. Enqvist, S. Nurmi, D. Podolsky, and G. I. Rigopoulos, *On the divergences of inflationary superhorizon perturbations*, *JCAP* **0804** (2008) 025, [[0802.0395](#)].

[50] I. Zaballa, Y. Rodriguez, and D. H. Lyth, *Higher order contributions to the primordial non- gaussianity*, *JCAP* **0606** (2006) 013, [[astro-ph/0603534](#)].

[51] C. T. Byrnes, K. Koyama, M. Sasaki, and D. Wands, *Diagrammatic approach to non-Gaussianity from inflation*, *JCAP* **0711** (2007) 027, [[0705.4096](#)].

[52] D. Babich, P. Creminelli, and M. Zaldarriaga, *The shape of non-gaussianities*, *JCAP* **0408** (2004) 009, [[astro-ph/0405356](#)].

[53] M. Haack *et. al.*, *Update of D3/D7-Brane Inflation on K3 x T2/Z2*, *Nucl. Phys.* **B806** (2009) 103–177, [[0804.3961](#)].

[54] L. Leblond and S. Shandera, *Cosmology of the tachyon in brane inflation*, *JCAP* **0701** (2007) 009, [[hep-th/0610321](#)].

[55] S. Renaux-Petel, *Combined local and equilateral non-Gaussianities from multifield DBI inflation*, [0907.2476](#).

[56] D. Langlois, S. Renaux-Petel, D. A. Steer, and T. Tanaka, *Primordial fluctuations and non-Gaussianities in multi- field DBI inflation*, *Phys. Rev. Lett.* **101** (2008) 061301, [[0804.3139](#)].

[57] D. Langlois, S. Renaux-Petel, D. A. Steer, and T. Tanaka, *Primordial perturbations and non-Gaussianities in DBI and general multi-field inflation*, *Phys. Rev.* **D78** (2008) 063523, [[0806.0336](#)].

[58] X. Gao and B. Hu, *Primordial Trispectrum from Entropy Perturbations in Multifield DBI Model*, *JCAP* **0908** (2009) 012, [[0903.1920](#)].

[59] X. Gao and F. Xu, *Loop Corrections to Cosmological Perturbations in Multi- field Inflationary Models: I. Entropy Loops*, *JCAP* **0907** (2009) 042, [[0905.0405](#)].

[60] N. Bevis, M. Hindmarsh, M. Kunz, and J. Urrestilla, *Fitting CMB data with cosmic strings and inflation*, *Phys. Rev. Lett.* **100** (2008) 021301, [[astro-ph/0702223](#)].

[61] M. Hindmarsh, C. Ringeval, and T. Suyama, *The CMB temperature bispectrum induced by cosmic strings*, [0908.0432](#).